DIRECT OBSERVATION OF DRYING BY NEUTRON AND X-RAY TOMOGRAPHY ANALYSIS

M. H. Moreira[(1)]*, S. Dal Pont[(2)], A. Tengattini[(3)], A. P. Luz[(1)], T. M. Cunha[(1)], R. F. Ausas[(4)], V. C. Pandolfelli[(1)]

[(1)] Federal University of Sao Carlos, Graduate Program in Materials Science and Engineering, Sao Carlos, SP, Brazil.
[(2)] 3SR, Université Grenoble Alpes, Grenoble, France.
[(3)] Large Scale Structures, Institut Laue-Langevin, Grenoble, France.
[(4)] Institute of Mathematical and Computer Sciences, University of São Paulo, São Carlos, Brazil.

ABSTRACT

The drying of refractory monolithics is one of the main drawbacks of this class of materials due to its implication on the production halt of many industrial equipment. This is especially true for calcium aluminate cement (CAC)-bonded castables, where the vapor derived from the unreacted water and dehydration reactions can pressurize yielding cracks and explosions of the ceramic lining. Numerous advances on additives have been made to increase these materials' resistance to explosive spalling, however, the fundamentals of the physical phenomena that yields such a problem remain an open issue. For years, the techniques used to study this process were limited to indirect tests, such as the thermogravimetric analysis or the pressure and temperature measurements of samples being unidirectionally heated. Recently, direct techniques such as nuclear magnetic resonance and X-ray tomography were applied in the context of regular concrete on fire scenarios. The current work presents preliminary results of neutron tomography applied to monitoring the drying of refractory castables. The overall behavior of the castable was qualitatively similar to those observed for regular concrete, and the results provide information that can be successfully applied on numerical simulations of larger pieces with dimensions closer to the industrial ones, overcoming the main drawback of such techniques, their small sample dimensions.

INTRODUCTION

Drying consists in the removal of water from a material via a gradient on the concentration, temperature or pressure distribution inside a porous medium[1]. Several mechanisms can act as a direct consequence of these inhomogeneities. The most notable examples are the convection mechanism due to the temperature gradient and the mass flux, which is related to a pressure difference (i.e., following the Darcy law).

Even though several studies were done[1,2], the highly dynamic nature of the drying stage, as well as the large sizes and masses of refractory pieces applied in industrial processes, still offer several challenges for the comprehension and, ultimately, the optimization of the drying performance of monolithics.

Studies using thermogravimetric analysis provided important advances on the understanding of the dehydration reactions that take place during the initial heating of castables[1, 3, 4]. These tests, however, do not provide any information on the moisture distribution inside the material, or the pressure values which are developed in their pores.

Additionally, several aspects need to be considered as well, such as the differences between the heating method used in the TGA furnaces and the ones in industrial process (i.e., heating from all sides or unidirectionally, using a gas burner or even microwaves), the size effects and the kinetics impact on the drying behavior.

One option that offers more information is by using sensors for the measurement of temperature and pressure evolution inside prismatic samples during unidirectional heating[5,6], such test is also known as PTM (pressure, temperature and mass measurement). This method was initially developed for studying regular Portland cement concrete under fire accidents[2] and it can be used to calibrate or even validate numerical models[5].

However, Dauti et al. [7] demonstrated, with the help of neutron tomography, that even very thin (0.25 mm in diameter) thermocouples are able to capture and stabilize air bubbles around themselves, when they are embedded in ceramic samples. Consequently, a large variation of pressure values is usually obtained during the measurements carried out with PTM tests, as reported in the literature[7].

The presence of sensors effectively changes the ceramic microstructure and the resulting collected data may not be representative of an unaltered material.

Direct imaging techniques became recently very promising, both for studying refractory and Portland cement concrete[3]. The most common techniques are the X-ray and neutron tomography, ground penetrating radar (GPR), or nuclear magnetic resonance (NMR), each technique displaying a different set of advantages and drawbacks inherent from the very nature of these methods.

Non-intrusive methods which don't rely on sensors such as neutron and X-ray tomography share the same principle. A beam of particles (in the case of neutrons) or electromagnetic waves (in the case of X-ray or ground penetrating radar) is directed towards the sample. Regions rich in water will interact differently from those that are dry and the resulting signal will reflect such differences.

Using multiple images obtained at a set of different angles (for the X-ray and neutron tomography) one can create images of the whole volume with the aid of a reconstruction algorithm. In the case of neutrons, this interaction is based on the scattering of neutrons by the hydrogen atoms comprising the water molecules[8].

The X-ray beam, on the other hand, interacts with the electrons of the atoms and, consequently, its capacity to differentiate between regions rich or poor in water is less efficient than the neutron tomography technique[8] (see Fig. 2 (d)).

Meanwhile, the ground penetrating radar approach relies on the fact that the electromagnetic waves propagating in a medium are reflected and scattered when a sudden change in electrical properties is found (which occurs when water is present). This approach is more feasible even for bigger samples than the ones used in the tomography-based techniques

These three techniques have in common the fact that the only information available is the relative change in water concentration at a given position.

On the other hand, nuclear magnetic resonance, which is based on the relaxation time of the nucleus of the hydrogen, can provide information on the configuration of the water molecules[9] (i.e., if they are on small or big pores). This comes at the expense of the capability of reconstructing the whole 3D domain.

Also, although possible[10], simultaneous drying and NMR analysis is challenging and prone to inaccuracies, as the heating elements

often have metallic parts which can interfere with the results and the relaxation time can be affected by the temperature[9]. A summary of the setup of these non-intrusive techniques used to study the drying is presented in Fig. 1.

It is clear from (a) that the main difference between X-ray and neutron tomography is the beam source, which is orders of magnitude more complex and more expensive for the latter as it relies on a nuclear reactor to provide the high intensity neutron beam. Also, from the setup of the NMR (b) and GPR (c), it is possible to see that the resulting data is essentially 1D.

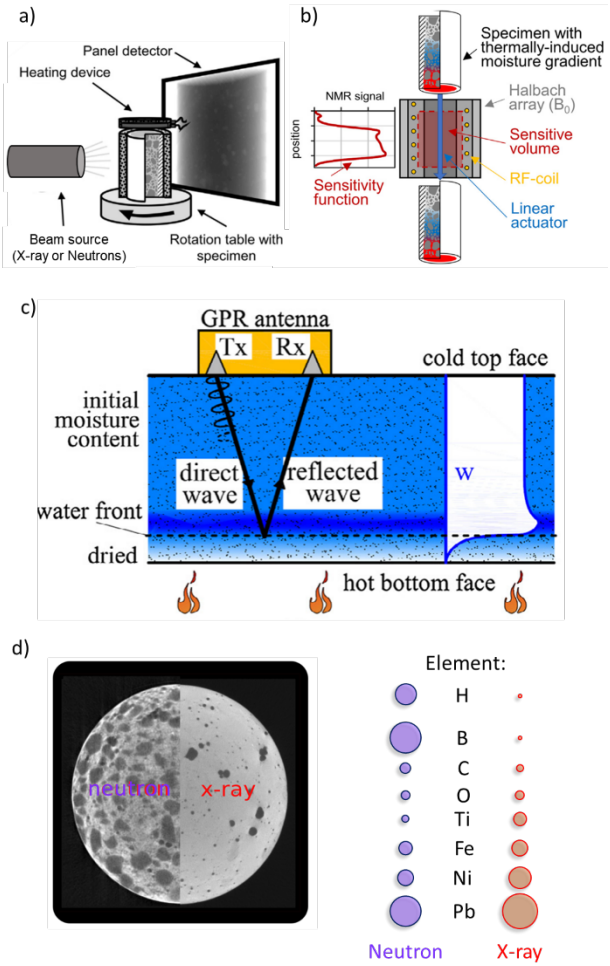

Fig. 1. Experimental layout of the imaging techniques, (a) is the setup of the X-ray or neutron tomography, (b) represents the nuclear magnetic resonance tests and (c) describes the function of the ground penetrating radar. The comparison between neutron and X-ray can be seen in (d), where the difference of interaction of each element with the different sources is also presented. Adapted from Stelzner et al.[9], Felicetti et al.[7] and Dauti et al.[8].

Finally, from Fig. 1 (d), it is evident that the higher scattering of neutrons by hydrogens results in a more pronounced contrast between the regions rich in water and dry areas, as seen from the radial slice.

Thus, the neutron tomography analysis was chosen to be applied for studying refractories castables as a complement to the works performed by Barakat et al.[9], which was based on using NMR.

Thus, the current study aims to present the very first (to the best of the authors' knowledge) direct observation of the drying in a refractory material using neutron tomography. This is an important advance as it can directly benefit the other two main fronts of development and studies of the drying of refractory castables: the numerical modelling and the industrial perspectives, as seen in Fig. 2.

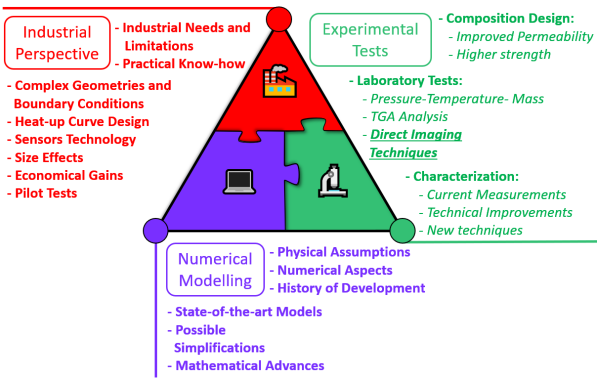

Fig. 2. The three main pillars on the study of the drying of monolithics. The current work is a fundamental advance on the experimental tests category, which can bring progress to both the numerical models and the industrial perspective.

MATERIALS AND METHODS

Neutron Tomography Tests

The experiments presented in the current work were performed on the NeXT equipment at the Institut Laue Langevin (ILL) with a final spatial resolution of 160 µm and a time interval between tomographies of only 58.5 s. Fig. 3 presents the layout of the experiment; further details can be found in Tengattini et al[11]. During the experiments an infrared radiator heater (Elstein HTS - High Temperature Heater) was placed on the top surface of the sample and its heating followed two distinct protocols: (i) the "slow heating" where the sample was heated with a 10 °C/min rate until reaching 500 °C and (ii) a "fast heating" of 158 °C/min rate until 500 °C (see Fig. 8).

A dense CAC-bonded refractory castable was prepared (Table 1) as described in Luz et al.[12]. The samples were cast in cylindrical PVC molds or in a sintered alumina ceramic casing with an inner diameter of 33 mm and a height of 50 mm, depending on the use or not of a casing during the neutron tomography test.

Table 1: 5CAC composition used in the neutron tomography tests based on the Andreasen's particle packing model with q = 0.21.

Raw materials		**Composition (wt.%)**
Tabular alumina	AT (d < 6)	74
Calcined and	CL370	11
reactive alumina	CT3000SG	10
Calcium aluminate cement	Secar 71	5
Distilled Water		4.5

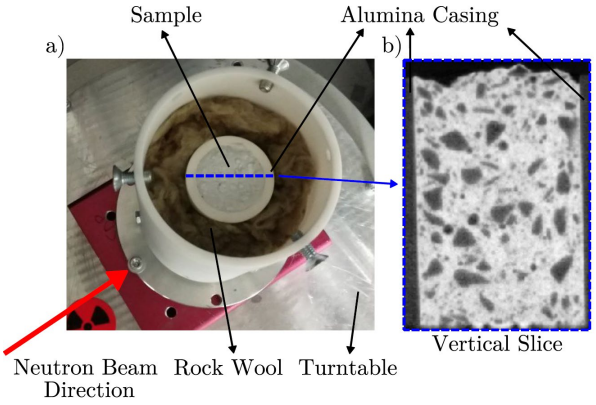

Fig. 3. (a) Layout of the neutron tomography test conducted in the NeXT equipment at Institut Laue Langevin (ILL) and (b) vertical slice of the reconstructed data.

Post-processing of the Results

The 3D representation of the samples was obtained using the Feldkamp filtered back projection and a commercial reconstruction software (X-act, by RX Solutions). The digital representation of the sample was composed of a set of 300 slices in the cylinder's height.

Even though several advanced calculations can be performed with the obtained data, the basic quantity used for the analysis in the current work was the relative difference, $\psi(\mathbf{x}, t)$, calculated by Equation 1.

$$\psi(\mathbf{x}, t) = \frac{\left(I(\mathbf{x}, t) - \hat{I}(\mathbf{x}, t_0)\right)}{\hat{I}(\mathbf{x}, t_0)} \times 100\% \quad (1)$$

where $I(\mathbf{x}, t)$ is the intensity of a voxel on position $\mathbf{x}$ ($\mathbf{x} = (\mathrm{x}, \mathrm{y}, \mathrm{z})$) at time t, and $\hat{I}(\mathbf{x}, t_0)$ is the voxel value at the reference state, which was defined to be the median of the first 10 tomographies, as described by Dauti et al.[8].

RESULTS AND DISCUSSION

Casing Effect Analysis

The first set of results describes the effect of a ceramic casing around the sample. This has several implications and can ultimately yield a truly unidirectional mass and heat transport inside the sample.

Dauti et al.[8] reported that a noticeable increase in the water content was observed ahead of the drying front when evaluating Portland cement concrete samples with no impermeable ceramic casings. However, it was not identified whether such increase were associated with real moisture accumulation or the *"beam hardening"* effect, which is the screening of more energetic neutrons by the hydrogen scattering on the water-rich positions, as it can mainly take place when lateral drying occurs.

Tengattini et al.[11], tried to use quartz and titanium as the enclosing casing, which was not successful. This might be related to differences in the thermal expansion of the casing and the sample, resulting in some air gaps at the materials interface from where water could still escape (see Fig. 5). Thus, the alumina ceramic casing used in this present work was specifically selected to match the characteristics of the 5CAC composition and result in a true unidimensional drying.

Fig. 4 describes the relative difference in water distribution for samples with and without the ceramic casing. Three main conclusions can be readily drawn from these results: (i) the drying front is completely flat when the sample is cast inside the alumina casing; (ii) the water accumulation is more evident in the sample inside the ceramic jacket and (iii) a secondary drying front is observed on the bottom of this sample.

This set of results is important and confirms some observations as well as juxtaposes others. First, the secondary drying is an important effect to be observed. Even in this case where the sample size is small, and numerical simulations indicate that the temperature gradient is around 17°C, this secondary drying is observed indicating that in real life applications, this can be an important way to guarantee a safe and efficient drying.

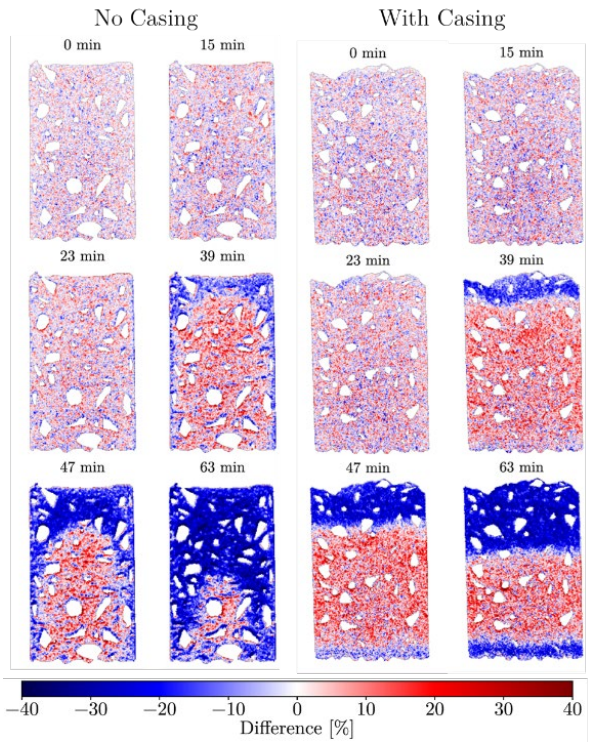

Fig. 4. Relative water content difference with respect to the initial state for samples with and without a ceramic casing for different time steps.

As a matter of fact, in industrial equipment containing ceramic linings, weepholes are often drilled on the metallic outer shells to allow water withdrawn, which often is observed as a liquid stream, or in some cases even as water jets.

The current findings are not in tune with the conclusions presented by Barakat et al.[10], as these authors only observed minor increases in the saturation content, and claimed that it could not be related to moisture clog, as the samples and the thermal gradients were too small.

As the NMR results can be spatially visualized, one can only infer that the procedures taken by Barakat et al.[10] to enforce the unidimensional drying were not enough, due to the different thermal expansion coefficient of the evaluated refractory castable and the PTFE beaker used as the casing for the NMR tests[10]. Fig. 5 shows the linear expansion

behavior of 5CAC castable and other materials that were used as casings during the drying measurements.

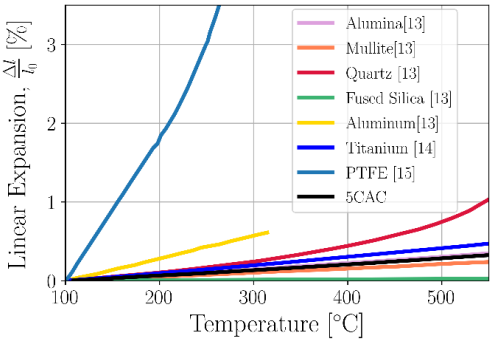

Fig. 5. Linear thermal expansion of common material candidates for casings of non-intrusive methods, the results are normalized from 100°C. Adapted from [13, 14, 15].

Moreover, the neutron tomography setup described herein can also be representative of a more realistic scenario, such as the refractory lining of a furnace. This is illustrated in Fig. 6, where the compatibility between a flat wall and the experimental setup is described by the specific boundary conditions.

This yields an important tool to not only explore alternatives to improve the efficiency of the drying of different compositions, but also to obtain a deeper understanding of the drying phenomenon.

Heating Rate Analysis

The second set of analysis was based on the comparison of the drying behavior of samples heated with different protocols. Two 5CAC samples were heated with a fast (158 °C/min) and slow (10 °C/min) rates until the heater temperature reached 500° C. The reason for these high heating rates was the limited time in the NeXT equipment. Further tests will consider heating rates closer to the ones found on the industrial application.

Fig. 7 presents the heating curves scheduled for the infrared heater, as well as the results of the relative difference in water content at different time steps.

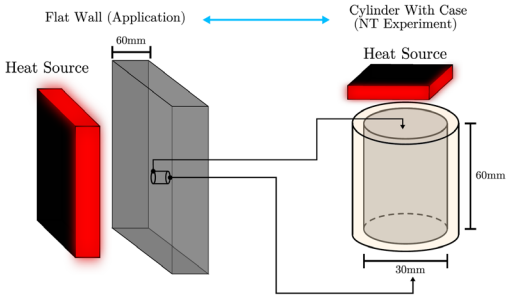

Fig. 6. The correspondence between the geometry and boundary conditions of a wall commonly found in the cases of interest, and the cylindrical neutron tomography sample with the ceramic casing.

It is evident that the drying starts earlier for the sample heated with the 158 °C/min rate, where a noticeable drying front was detected with just 15 minutes of test, when the heater temperature is already at 500 °C. On the other hand, the slow heated sample only shows a drying front at the 39 minute mark, when the temperature is still at 425 °C.

At the same time stage, the fast heating procedure starts to show the development of a secondary drying front at the bottom of the sample. This is only clear on the slow sample at the 47 minute mark.

Most surprisingly is the fact that the final result at the end of the test is close for both heating conditions. This suggests that the temperature increase of the sample was probably the limitating factor, specially when the heater reached the plateau stage and the thermal conductivity became the regulating factor for the thermal energy transport.

This result was also observed when the evolution of the mean relative difference of specific sub volumes of the sample were plotted, as shown in Fig. 8.

The top slice behavior confirms that the heating starts earlier for the fast heating. The water release rate increases until a distinct peak is reached around the 23 minute mark.

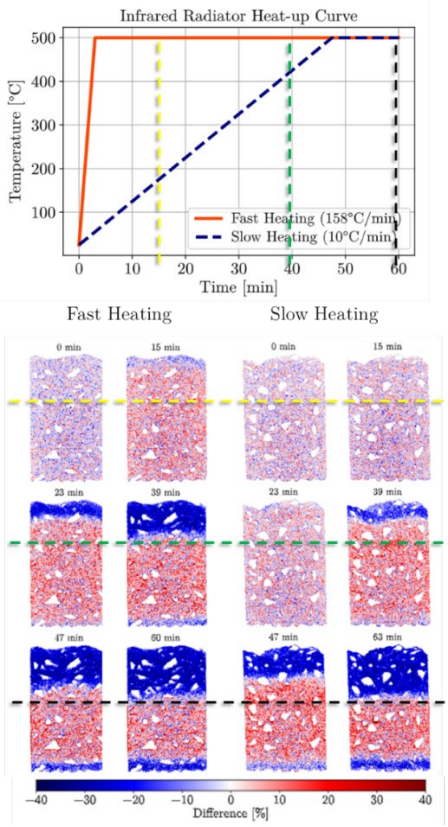

Fig. 7. Relative water content difference with respect to the initial state for the samples heated using the fast and slow protocols. The dashed lines can be used to infer the temperature distribution on the sample by the infrared's temperature.

This might be related to the dehydration reactions occurring at this position. After that, the water removal rate stabilizes around the 0.15 %/min, until the end of the experiment (also shown by the linear behavior, with $r^2 = 0.99$).

For the slow heating, the behavior is similar but delayed, with the maximum peak taking place around 41 minutes. This is a strong indication that this peak is in fact related to a thermally activated chemical reaction of dehydration. After this event, the drying rate decays until reaching a constant stage. Nevertheless, it is interesting how the water removal rate is considerable higher, around 0.45 %/min.

The reason for this later faster water removal, for the sample that was heated slowly, might be related to the presence of the temperature plateau. If, for instance, the final temperature was the common operating temperature found in the industry, it is believed that the sample heated by the fast protocol would finish its drying earlier.

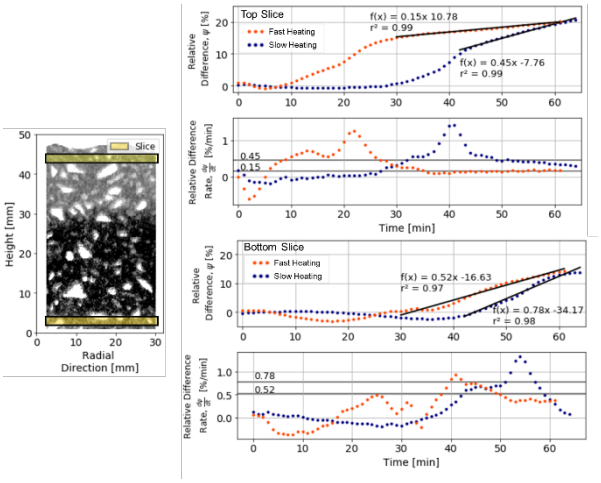

Fig. 8. Evolution of relative difference for top and bottom slices of the sample and the respective rates for the slow heating and fast heating cases.

Further studies with temperature measurements and with longer heating protocols are necessary to further understand this unexpected behavior. Nonetheless, these findings highlight the complexity of designing heating schedules and how the temperature plateaus need to be well understood and justified to promote safer drying process.

CONCLUSIONS

The drying of refractory castables is a complex subject which requires interdisciplinary efforts, ranging from numerical methods, experimental techniques and knowledge of the industrial perspective. Advanced non-intrusive techniques originally applied to Portland cement concrete can provide unprecedented findings. In the current

work the use of neutron tomography yielded a new method to study the castable drying.

The use of a ceramic casing completely altered the dynamics of water removal. The presence of a secondary drying front was also detected for the sample inside the casing, which displayed a pronounced moisture accumulation ahead of the drying front. When comparing two different drying rates, it was possible to see that using a temperature plateau led to similar final water content.

The framework proposed herein can be further enhanced by using thermocouples to obtain simultaneously the temperature profiles and the moisture distribution, or by using longer heating protocols, that better represents the industrial scenario.

ACKNOWLEDGMENTS

This study was financed in part by the Coordenação de Aperfeiçoamento de Pessoal de Nível Superior - Brasil (CAPES) - Finance Code 001. The authors thank the Fundação de Amparo à Pesquisa do Estado de São Paulo - FAPESP (grant number: 2021/00251-0 and 2019/07996-0), The authors are greatly thankful for FIRE support in this work.

REFERENCES

1. A.P. da Luz, M.A.L. Braulio, V.C. Pandolfelli, Refractory Castable Engineering, vol. 756, Goller Verlag GmbH, (2015)
2. Moreira, M. et al. Main trends on the simulation of the drying of refractory castables - Review. Ceramics International, Elsevier, vol. 47 [20] pp. 28086-28105 (2021)
3. A. P. da Luz et al., Drying behavior of dense refractory ceramic castables. Part 1– General aspects and experimental techniques used to assess water removal. Ceramics International, Elsevier, vol. 47 [16] pp. 22246-22268 (2021)
4. G. Palmer, et al. The accelerated drying of refractory concrete – Part 1: a review of current understanding, Refractories Worldforum 6 [2] pp 75–83 (2014)
5. K.G. Fey, et al., Experimental and numerical investigation of the first heat-up of refractory concrete, Int. J. Therm. Sci. [100] pp. 108-125, (2016)
6. P. Meunier, et. al, Methods to assess the drying ability of refractory castables, UNITECR 2013, pp.1–4 Kyoto, Japan. (2013)
7. Shen et al., On the moisture migration of concrete subject to high temperature with different heating rates, Cement and Concrete Research, [146], pp. 106492, (2021)
8. D. Dauti, A combined experimental and numerical approach to spalling of high performance concrete due to fire, Université Grenoble Alpes, (2018)
9. L. Stelzner et al., Thermally-induced moisture transport in high-performance concrete studied by X-ray-CT and 1HNMR, Construct. Build. Mater. pp. 600–609 (2019)
10. A.J. Barakat, et al., Direct observation of the moisture distribution in calcium aluminate cement and hydratable alumina-bonded castables during first-drying: an NMR study, J. Am. Ceram. Soc. pp. 2101–2113 (2020).
11. A. Tengattini, et al., Quantification of evolving moisture profiles in concrete samples subjected to temperature gradient by means of rapid neutron tomography: Influence of boundary conditions, hygro-thermal loading history and spalling mitigation additives, Strain [56] pp. 12371, (2020)
12. A.P. Luz, et al., Drying behavior optimization of dense refractory castables by adding a permeability enhancing active compound, Ceram. Int. pp. 9048–9060 (2019)
13. M. W. Barsoum, Fundamentals of ceramics, McGraw Hill, New York, (1997)
14. P. Hidnert, Thermal expansion of titanium, J. Res. Natl. Bur. Stand [30] pp. 101 (1943)
15. Characteristics of Fluororesins, Valqua LTDA, Available On-line on http://www.seal.valqua.co.jp/en/fp_property/fluoroplastics_characteristic/